Lifespan driven reorganization of the global network dynamics unfold on a multifrequency landscape

Bikash Sahoo[1]; Anagh Pathak[1**]; Gustavo Deco[2], Arpan Banerjee[1*]; Dipanjan Roy[1*]**

[1] Cognitive Brain Dynamics Lab National Brain Research Centre (NBRC), NH8 Nainwal Mode 122051 Manesar, Haryana, India

[2] Institució Catalana de la Recerc Estudis Avançats (ICREA), Universitat Pompeu Fabra, Passeig Lluís, Companys 23, Barcelona, 08010, Spain

**** Equal contributions**

***corresponding authors**

dipanjan.nbrc@gov.in; arpan@nbrc.ac.in

Keywords: Healthy Ageing, Peak Alpha, Global coherence, Metastability, Multifrequency

Abstract

Cognitive processes are mediated by communication among multiple brain areas that individually exhibit oscillatory neuro-electromagnetic signals emerging from a cascade of complex physiological processes. Several studies have reported that aging changes the intrinsic properties of neural oscillations, both in resting state and in the context of cognitive tasks. For example, the amplitude of resting and motor-related beta band oscillations (16-25 Hz) is typically found to be higher in the older population compared to the younger population. Similarly, a substantial number of reports have highlighted that peak alpha frequency (8-12 Hz) is lowered in neurodegenerative disorders and in healthy aging. How such observations emerge from underlying neuronal signal processing mechanisms remains elusive. Furthermore, how do the spatiotemporal organization of these rhythms support the current neurobiological theories of aging is poorly understood. Here we addressed these issues using the resting state magnetoencephalogram (MEG) data from a large cross-sectional cohort consisting of 650 human participants with age range 18-90 covering the entire adult lifespan. Concurring with previous research in

smaller cohorts, we found a consistent increase in the power of beta oscillations and a decrease in the peak alpha frequency as a function of age. Subsequently, we found significant posterior to anterior shifts in the spectral topographies of both alpha and beta bands. To reconcile these observations with a comprehensive theory at the level of network level signal processing, we computed the whole-brain global coherence that captures the degree of communication among nodes of a large-scale network as a function of aging. The global coherence among MEG signals increased with age in slower time-scales i.e. delta (1-3 Hz) and theta (3-7 Hz) frequencies. Simultaneously, global coherence decreased for faster timescales i.e. alpha (8-12 Hz) and beta (16-25 Hz) frequencies. Further, using the measure of metastability that quantifies the divergence of a network from a stable synchronous state, we characterized the dispersion of information processing in different frequency bands. Putting together, our study reveals how neurobiological theories of aging such as posterior to anterior shifts of sensory and cognitive processing, dynamic workspace hypothesis can all be reconciled using resting-state MEG data. We could highlight how the temporal structure of MEG signals is representative of a more comprehensive understanding of large-scale network mechanisms that govern lifespan dynamics.

Introduction

Healthy Ageing and Temporal Structure

A comprehensive understanding and characterization of the process of healthy aging are essential to treat age-associated neurological impairments such as Alzheimer's and Parkinson's disease. Till date, there is no comprehensive theory of healthy aging that explains the role of neuronal mechanisms at various temporal and spatial scales. Neuronal oscillations observed in EEG/ MEG data are essential markers of cognition (Buzsaki 2011), and researchers overwhelmingly agree on the use of field potential to tap neuro-cognitive processes associated with human brain function (Pesaran et al., 2018) and in particular aging (Ishii et al., 2017). The frequency domain representations can capture the presence of state space in the information processing sense, and subsequently the modes of communication or interactions among constituent functional units. Using the language of physics, a large-scale complex system such as a brain, transitions among various states of organization (order), sometimes defined by the temporal relationships (such as coherence) among spatially segregated regions (Hipp et al., 2012). On the other hand, the propensity of the brain states to move away from states of order can be captured by "metastability", a quantitative marker to define how far any physical system is away from "order" and how strong the tendency is there to come back to an ordered state (Naik et al. 2017). The fundamental objective of this article is to

illustrate that these processes can be interpreted from neurophysiological data (MEG) obtained from a large cohort of a healthy aging population (Taylor et al., 2017).

A large portion of research seeking to map healthy aging-related behavior on to modulation of neural oscillations has taken the factor of age as a binary variable, i.e. comparing young versus old (e.g., Strunk et al., 2017). While it is essential to know what changed between younger and older populations when these network dynamic alterations begin to manifest in the lifespan trajectory remains elusive. Critical stages may exist during development when significant changes occur to brain dynamics (Koenig et al., 2002). The steps mentioned above might also hold for the process of healthy aging, hence tracking down the lifespan changes to the temporal structure of brain signals holds a lot of promise.

Why are frequency specific changes relevant parameters to study aging?

Quantification of coordinated synchrony among neural populations via spectral measures has been shown to be pertinent to cognition and their decline in neurodegenerative and developmental disorders (Alderson et al., 2018; Uhlhaas and Singer, 2006; Fries, 2005; Bressler, 2001).

In aging literature a widely reported marker is the slowing down of alpha rhythms in mild cognitive impaired and Alzheimer's affected population (Babiloni et al., 2006; Garces et al., 2013). Nonetheless, the large-scale network mechanisms behind the slowing of alpha and its decreasing power with aging are as an open question (see Ishii et al., 2017 for an excellent review). For example, what is the relevance of slowing brain rhythms to the dynamic repertoire of the developing brain and essential brain functions? Such questions require using various measures of signal and physiological complexity from neuroimaging data obtained from MEG, EEG & fMRI.

Current Mechanistic Insight and our Approach

Aging is known to be accompanied by a decline in the structural connectivity among brain regions (Raz et al., 2005; Pfefferbaum et al. 2000; Davis et al., 2009). Recent research has suggested that a compensatory mechanism emerges with aging, that try to counteract the deleterious effects of the losses as mentioned above (Davis et al., 2008; Reuter-Lorenz et al., 2000). All the change mentioned earlier are related to a reorganization of brain networks with increasing age in the lifespan trajectories (Deco et al., 2017; Naik et al., 2017). This reorganization of brain networks can be expected to

play a pivotal role in changing the spatiotemporal properties of neuronal oscillation and the variability of the global communication states (empirically characterized by coherence and metastability) along lifespan trajectories.

Resting-state magnetoencephalogram (MEG) recordings from the Cambridge-Ageing Neuroscience (Cam-CAN) group offers us a unique opportunity to capture the organizational features empirically and tying it up to a broader theoretical framework (Taylor et al., 2017)

Here we provide empirical evidence of reorganization of the brain on the sensor level along with changes in characteristic properties of slow (integrative) and fast (segregative) neural oscillations with aging. Since this analysis has been carried out on a large cohort of an aging population(cross-sectional) to understand lifespan trajectories, the findings can be considered to be highly robust and reliable. Besides, they help in providing insights into lifespan related critical stages of healthy aging as well.

Results

For majority of analysis carried out in this work, we have considered age to be a continuous variable. However, for certain analysis we have divided the age values of total N=650 subjects into four age groups (Young Adults (YA), Middle Elderly (ME), Middle Late (ML), Older Adults (OA)), for which the demographic information has been provided in **table 1**.

Spectral properties of neural oscillations with aging

We started with spectral estimation of the resting state data to investigate the effect of healthy ageing on the fundamental properties of the endogenous band-limited neural oscillations such as amplitude and center frequency. Since the Head Position Indicator (HPI) coil related noise can be unreliable at higher frequencies we concentrated our analysis between 0-40Hz which fully contains the neural oscillations in the Delta(<4Hz), Theta(4-8Hz), Alpha(8-12Hz), and Beta(16-25Hz) frequency bands.

Figure 1A shows the average global spectrum of four different age groups. Qualitative changes can be seen in the spectrum among age groups in both Alpha and Beta oscillations. A gradual increase in Beta band power was seen with increase in age and a shift in the peak Alpha frequency (PAF) was observed between the youngest and oldest

age group. Motivated by these qualitative results we further sought to quantify the statistical significance of ageing related difference and possible neural implications of these changes in the spectrum of Alpha and Beta band oscillations.

Alpha band power was estimated by averaging the estimated spectral values within 8-12 Hz. Estimated Alpha band powers were grouped according to the four age groups. Since the number of subjects within each age group were not uniform, for further statistical comparison between two groups we always chose the minimum number of subjects among the age groups i.e. 126 for the YA group. We randomly sampled 126 values from each group and performed unpaired t-test. The sampling was iterated over 5000 times. Correction was made for multiple comparison using False Discovery Rate procedure (Benjamini and Hochberg, 1995). Using Kruskal-Wallis test, we did not find any significant difference in alpha power among age groups (p = 0.991). Performing t-test among any two groups for alpha power didn't show any significance either.

Beta band power was estimated by averaging the estimated spectral values within 16-25 Hz. Beta powers were grouped into four age groups and similar statistics were performed as explained in the previous subsection. **Figure 1B** shows variation in beta power among four age groups. We found significant effect of age on beta band activity ($R^2 = 0.04, P < 0.001, N = 650$). Significant difference were seen between age groups YA, 18-35 years and ME, 36-50 years (t(250) = -3.55, p = 0.001), groups YA and ML, 51-65 years (t(250) = -4.51, p < 0.001), groups YA and OA, 66-88 years (t(250) = -5.60, p < 0.001) and a marginally significant difference was observed between groups ME and OA (t(250) = -2.05, p = 0.070). Spearman's rank correlation between age of the individual and beta power was found to be 0.216, p < 0.001, which suggests beta activity increases with aging.

Peak Frequency shift for alpha band: Spatiotemporal Organization

Frequency value at which there was maximum activity in the alpha band i.e. 8-12 Hz for a subject, was taken to be the peak alpha frequency of that subject. **Figure 1C** is an age-spectrogram which shows variation in the power spectral density in the alpha band with age. Age values were grouped into bins of 5 years starting from 18 years. The bins were non-overlapping and the center of each bin was considered as the representative age value of the bin. We found significant effect of age on center alpha frequency ($R^2 = 0.14, P < 0.001, N = 650$). Spearman's rank correlation between age and center frequency in the alpha band was found to be -0.384 (p < 0.001).

Further we investigated the variation of peak alpha frequency with aging at individual sensor level. **Figure 1D** shows the topographical map of Spearman's rank correlation between peak alpha frequency and age. Overall, peak alpha frequency decreased with age in many sensors and had a statistically significant negative correlation with age. Surprisingly, a set of sensors in the prefrontal cortex did not show a robust decrease in peak alpha frequency with age. In these sensors, either the correlation was low or nonsignificant (Spearman's rank correlation, -0.0248, p=0.5284).

Whole brain measures of neuronal communication states during ageing

Presence of large-scale functional brain networks was investigated using global coherence across all MEG sensors at different frequencies for each subject (Cimenser et al., 2011; Kumar et al., 2016). **Figure 2** shows the average of the global coherence spectrum for the four age groups. Qualitative differences were observed across frequency range 0-25 Hz, which were quantified and tested for statistical significance.

Global coherence at all the frequency values within a frequency band were averaged to generate a representative value for the corresponding frequency band in four age groups, YA, ME, ML, OA (Fig 1A). In order to track lifespan trajectories, subjects were grouped into finer non-overlapping age bins of 5 years between 18-88 years. Representative global coherence in age bin was averaged and standard error was computed for each age bin (Fig 2B).

We observed that the global coherence in Delta band, 1-3 Hz ($y = 0.0006x + 0.2863, R^2 = 0.077, p < 0.001, N = 650$), in Theta band, 3-7 Hz ($y = 0.0004x + 0.2583, R^2 = 0.063, p < 0.001, N = 650$), and Alpha band, 8-12 Hz ($y = 0.0013x + 0.4168, R^2 = 0.076, p < 0.001, N = 650$) was correlated with age. Correlation of age with global coherence in Beta band (16-25 Hz) was small ($y = -0.0002x + 0.2584, R^2 = 0.021, p < 0.001, N = 650$). Thus, we suspected that age had a differential effect vis-a-vis global coherence depending on the time scale of the oscillations. To test our hypothesis that age-related reorganization results in differential processing in slower and faster time scales we have further divided the oscillations into two major groups i.e. of slow time scale (1-5 Hz) and of fast timescale (10-20 Hz). As expected from the previous set of results we found significant increase in global coherence with increase in age for slow oscillations (Spearman's rank correlation $c = 0.248, p < 0.001$) and a significant decrease with aging in fast oscillations (Spearman's rank correlation $c = -0.356, p < 0.001$). 2-way ANOVA test revealed an age effect $F(1,3) = 4.74$, $p = 0.0027$, a frequency effect of $F(1,3) = 174.79$, $p < 0.001$ and an interaction effect of $F(1,9) = 9.23$, $p < 0.001$.

Topographical segregation of neural oscillations at different time-scales with aging

Next, we investigated the spatial boundaries of whole brain networks corresponding to age-related difference along slow and fast time scales of neuronal signal using subspace analysis borrowed from linear algebra. The key findings confirm our hypothesis that the topographical changes of the spectral power with aging i.e. the changes on the scalp level representation of Alpha and Beta band activity increases with age. Here, for simplicity, we considered only the two extreme age groups i.e. YA (18-35) and OA (66-88). **Figure 3A** shows the average topographical map of alpha activity at the center alpha frequency and average beta activity in 16-25 Hz for the youngest and oldest age groups. Performing cluster-based permutation statistics revealed statistically significant patterns of difference in alpha and beta band activity between the two age groups.

Although, we observed similar patterns of difference between the oldest and youngest age groups for global alpha band power and beta band power, there seemed to be a qualitative difference in the overlap of sensors representing alpha activity and beta band activity. We quantified the overlap between these two sensor topographies by the angle between their respective vector representations. Larger angles indicated more separation and less topological overlap between sensor groups.

We found significant effect of age on the angle between Alpha and Beta band activities' sensor wise representation ($R^2 = 0.056, p < 0.001, N = 650$). **Fig 3C** shows how angular separation of subspaces between scalp topographies from underlying alpha and beta frequencies increase as a function of age. Significant difference was found between age groups 18-34 and 51-65 (t(228) = -2.89, p = 0.011), age groups 18-34 and 66-88 (t(228) = -4.64, p < 0.001) and age groups 35-50 and 66-88 (t(228) = -3.42, p = 0.003).

Metastability and aging

We estimated the variability of neuronal communication states using metastability as a function of age and frequency. We observed a dichotomous pattern in metastability as a function of frequencies in all age groups, a sharp decrease with increasing frequencies till 12 Hz and a gradual increase in the metastability indices across frequencies between 12-40Hz (Fig 4). This was further confirmed by treating age as a continuous parameter and also by chunking participants in 4 age-groups as highlighted in previous subsections.

To identify the statistical trends, we grouped the participants in 4 age groups and performed t-test across the age-groups. Statistics similar to the power analysis was performed to confirm the correlation of age and metastability. Subjects were divided in

four age groups and unpaired t-tests were performed by drawing 5000 samples from each age group. Every random draw consisted of subjects equal to the smallest age group (126, Young). Resulting p-values were corrected for multiple comparisons by using the procedure described in (Benjamini-Hochberg,1995) and implemented using MATLAB functions. The following p-values and t-statistics were obtained for metastability in alpha band- YA vs ME (*p=0.07, t = -1.97*), YA vs ML(p<0.001, t= -4.52), YA vs E(*p<0.001,t=-4.332*), ME vs ML(*p= 0.0220, t= -2.5646*), ME vs E(*p=0.0284,t=-2.445*), ML vs E(*p=0.7542, t= -0.1703*). A 2-way ANOVA test revealed a age effect F(1,3) = 64.41,p ~ 0, a frequency effect of F(1,7) = 35.61, p ~ 0 and a interaction effect of F(1,21) = 2.08, p = 0.0027.

Differential profiles of slow vs. fast scales of metastability in aging

Our findings suggest a characteristic U-shaped profile of metastability as a function of various frequency bands. Interestingly, the minimum metastability was observed in the alpha frequency band, consistent across age groups (see Fig. 4). The comparison of metastability in slow and fast time scales across age-groups revealed an interesting inverse trend. The metastability associated with slower time scales (Delta and Theta) was found to be lower than the corresponding values for the faster time scales (Beta 4,5) in the young cohort (p<0.001) whereas the opposite trend was observed in the elderly group (p=0.0075)). This was further confirmed by pooling the metastability values of the slower and faster time scales together and performing non-parametric statistical tests (two sample Kolmogorov-Smirnov test (KS-test)).

Region Wise analysis of metastability reveals differential trends

In order to track changes in metastability in specific brain areas we segmented the sensors in 5 groups - Frontal, Centro-Parietal, Occipital, Left Temporal and Right Temporal regions. The region-wise analysis consisted of 14 randomly sampled sensors in each brain region. Next, we calculated region-wise metastability and tracked its change with aging. Spearman rank correlation was performed to characterize trends in band and region specific metastability.

This suggests that whereas Alpha band displays an increasing trend with age for all brain regions, Delta and Theta oscillations either stayed invariant or reduced as a function of age in the occipital, left temporal and right temporal regions. Beta band metastability showed the highest age correlation (using Spearman rank test) in the centro-parietal sensors while staying invariant in the occipital and temporal sensors.

The following Spearman rank coefficients were obtained for delta band - frontal (*c=0.2499, p<0.001*), centro-parietal *(c=0.1629, p<0.001*), occipital (*c=-0.0686, p=0.0805*), left temporal (*c~0, p=0.92*), right temporal (*c=-0.1428, p<0.001*). The corresponding values for alpha band were frontal (c=0.2161, p<0.001), centro-parietal (*c=0.1808, p<0.001*), occipital (*c=0.1348, p<0.001*), left temporal (*c=0.2030, pval<0.001*), right temporal (*c=0.2070, p<0.001*). For theta band- frontal (*c=0.1725, p<0.001*), centro-parietal (*c=0.2049, pval<0.001*), occipital (*c=-0.1141, pval=0.0036*), left-temporal (*c=-0.04, p=0.2396*), right-temporal (*c=-0.0457, p=0.2443*) were obtained. We tracked metastability in the beta band for three frequency bands ($\beta_1, \beta_3, \beta_5$) using similar statistical methodology. Centro-parietal sensors showed the highest age-related positive correlations (c=0.2046, 0.2542, c=0.1734, p<0.001 for the three bands respectively).

Discussion

Our results indicate distinct changes in spectro-temporal features of resting state MEG with aging. In this section, we relate our findings to existing literature and discuss their possible implications for the understanding of the process of normal and abnormal aging.

We report a significant age-related decline in peak alpha frequency. The decrease in peak frequency of alpha band has been reported to be a biomarker of normal and pathological aging process, especially for dementia, mild cognitive impairment, and Alzheimer's disease (Scally et al., 2018; Dickinson et al., 2018; Osipova et al., 2005; Jeong, 2004). Patients with Alzheimer's disease show a significant decrease in peak alpha frequency (PAF) compared to age-matched control group (Osipova et al., 2005; Jeong, 2004). Parkinson's patients with dementia have a lower PAF compared to age-matched controls (Soikkeli et al., 1991). While earlier studies suggest that PAF can be considered to be a robust biomarker of pathology, we observe very similar results in healthy aging as well. Neurodegenerative pathologies like AD and Parkinson's share many similarities with healthy aging, due to which many have speculated whether neurodegeneration is an accelerated aging process (Ciryam et al., 2016). The relationship between specific symptoms of pathologies such as Alzheimer's, Dementia and Parkinson's are hinted by some recent literature. Samaha et al. (Samaha et al., 2015) have demonstrated that individuals with higher PAF during eyes-closed resting state also showed a significantly finer temporal resolution in visual perception task and enhanced task performance. Taken together our finding of a shift of PAF with aging could serve as a possible predictor for age-related decline in perceptual acuity in a number of tasks. Interestingly, the same study also reports a weak but non-significant correlation between eyes-closed resting state PAF and age, further corroborating our findings of an age dependent shift in PAF.

Similarly, previous studies (Clark et al. 2004) have reported a significant reduction in working memory performance in digit span task with aging, while also reporting a positive relationship between PAF and working memory.

An analysis of topographical differences in PAF distributions between pathological and age-matched non-pathological populations can shed light on the differences between neurodegenerative processes and healthy aging. Our observation that a subset of frontal sensors doesn't show a significant decline in PAF forms the basis of this belief. We interpret these results in light of recent literature that reports an age-related reduction of inhibition in the prefrontal cortex of humans and rhesus macaques which leads to increased neural activity. This compensatory mechanism could underlie our observation of preservation of peak alpha frequency in frontal sensors and as such, could be an index of neuro- compensation (Bishop et al., 2010; Loerch et al., 2008). We also observe a distinct posterior to anterior shift in the spatial topography of the central power of spontaneous alpha activity with age. This assumes critical importance in light of recent literature that suggests that the topographical distribution of alpha band power can track spatial working memory (Foster et al.,2015). Additionally, the scalp topography underlying alpha band power has also been shown to predict the focus of covert spatial attention (Samaha et al., 2016). To our knowledge, ours is the first study that reveals age-related changes in spatial topographies underlying PAF power.

Beta oscillations are present in primary motor cortex at rest and get suppressed during movement (Pfurtscheller and Lopes de Silva, 1999). Beta oscillations in motor cortex are thought to be an index of motor inhibition and volitional movement (Heinrichs-Graham and Wilson, 2016). Research also suggests that an increase in intra-cortical GABAergic inhibition gives rise to an increase in resting state beta activity (Hall et al., 2011; Muthukumaraswamy et al., 2013). From this perspective, an increase in beta oscillations in the older population compared to the younger population can be reflective of increased motor inhibition (Heinrichs-Graham et al., 2018). Increase in the band-limited beta power in older population compared to younger population has been reported both in the context of resting state and sensory-motor task (Rossiter et al., 2014; Heinrichs-Graham and Wilson, 2016) and empirically demonstrates a mechanism by which healthy brain compensates for age-related increases in spontaneous beta activity by increasing the strength of beta oscillations within the motor cortices which, when successful, enables normal motor performance into later life (Heinrichs-Graham et al., 2018). We also observed the increase of beta band power with aging (Fig 1. B). As with alpha band, we observe a posterior to anterior shift in the topography of beta power with aging. Further, it has been reported that resting state band limited activity in slow frequency oscillations, i.e. delta and theta band is typically higher in younger population compared to older

population (Volf and Gluhih, 2011). However, we did not observe this on a global level in the present study.

According to a dominant view in neuroscience, coherent activity across neuronal assemblies is a hallmark of neuronal communication. This view holds that interareal coherence presents windows of excitability where communication channels between brain regions are maximally utilized (Fries, 2005). Resting state brain activity is said to reflect the brain's tendency to engage and disengage these channels of communication spontaneously (Deco et. al, 2011).

From a dynamical perspective, spontaneous brain activity must exhibit metastable dynamics, whereby the global brain dynamics stay clear of the two extremes of constant synchronization and desynchronization and instead, periodically shuttles back and forth between coherent and incoherent regimes. More formally, global coherence indexes the average phase and amplitude correlation across sensors whereas metastability measures the variability in phase relationships of sensors across time. The complimentary, yet related nature of global coherence and metastability offers unique insights into the mechanistic underpinnings of global brain dynamics. An example of this is a recent computational study by Vasa et al. which describes how local lesioning in nodes with high eigenvector centrality leads to a simultaneous decrease in global synchrony along with an increase in metastability. (Vasa et al., 2015). For a review of the complementary nature of global coherence and metastability, see (Deco et al. 2017, Hellyer et al. 2015, Vasa et al. 2015). It is evident how spontaneous metastable brain dynamics would contribute to cognitive flexibility. Since healthy aging exhibits complex changes in cognitive flexibility, we postulated changes in the brain's metastable dynamics as it ages.

We observe that alpha band exhibits the lowest metastability of all bands studied across all age groups. Interestingly, the alpha band also demonstrates the highest global coherence in any given age group, but whereas alpha metastability increases with age, alpha global coherence reduces with age. Taken together, this would strongly suggest the presence of a primary generator of alpha activity that aids in the maintenance of a brain-wide correlated network. The thalamocortical circuitry has long been regarded as the primary generator of activity that falls in the alpha band. Interestingly, a somewhat different trend is seen in the delta and theta band, where we notice an age-related increase in global coherence and metastability. Interestingly, we also notice inflection points in the life span profiles of global coherence around the age of 20-30 and 70-80 in both the slower and faster bands.

We observe an age-related increase in global metastability across all frequency bands under study here. Moreover, our results reveal a differential profile of relative metastability in the slower and faster frequencies as a consequence of aging. We want to discuss these results in the light of two opposing theories of healthy aging. The method of neuro-compensation argues that age-related changes in brain dynamics suggest a compensatory mechanism by which function gets restored in response to structural decline (Naik et al. 2017). In this regard, it is interesting to note that Alzheimer's disease and Traumatic brain injuries are associated with a reduction in global metastability (Córdova-Palomera et al., 2017; Hellyer et al., 2015). Since metastability is a direct measure of the functional capacity of the brain and has been shown to confer cognitive flexibility in task-switching, information-processing and logical memory (Hellyer et al. 2015), this would argue in favor of a compensatory explanation of the global increase in metastability with aging. In a similar vein, the differential profiles of metastability in the younger and older group would signify an age-related reorganization of brain networks, leading to a separation of temporal scales in cognitive processing. However, the neural noise hypothesis of aging would suggest a different interpretation. This theory argues that age-related cognitive decline is best explained as a consequence of an increase in the noisy baseline activity of the brain (Voytek et al., 2015; Dave et al., 2018). According to this framework, global phase inconsistencies would arise as a result of an age-related increase in neural noise. Within this framework, changes in global metastability and coherence reflect an epiphenomenon that occurs due to an increase in neural noise. Future efforts should focus on resolving this debate. One possible direction would be to study brain signals through measures of signal complexity using source reconstructed EEG/MEG, to elucidate the role of specific brain regions in bringing about metastable patterns of activity. Another promising avenue would be to invoke whole brain computational models which incorporate neural plasticity mechanisms that operate at time scales that are relevant to aging (Abeysuriya et al., 2018).

Methods

Subject details

Cam-CAN is a multi-modal, cross-sectional adult life-span population-based study. The study was approved by the Cambridgeshire 2 Research Ethics Committee, and all participants have given written informed consent. The data presented here belonged to Stage 2 of the study. In Stage-1, 2681 participants had been home-interviewed and had gone through neuropsychological assessments and been tested for vision, balance, hearing and speeded response. Participants with poor vision (< 20/50 on Snellen test), poor hearing (threshold greater than 35 dB at 1000 Hz in both ears), past history of drug abuse, with any psychiatric illness such as bipolar disorder, schizophrenia, with

neurological disease e.g. epilepsy, stroke, traumatic brain injury, or a score less than 25 in Mini-Mental State Examination were excluded from further behavioral and neuroimaging experiments. 700 participants had been screened from Stage 1 to Stage 2, of which Magnetoencephalogram (MEG) data from 650 subjects were available.

Data acquisition

Data used in the preparation of this work were obtained from the CamCAN repository (available at http://www.mrc-cbu.cam.ac.uk/datasets/camcan/) (Taylor et al., 2016, Shafto et al., 2015). For all the subjects, MEG data were collected using a 306-sensor (102 magnetometers and 204 orthogonal planar magnetometers) VectorView MEG System by Elekta Neuromag, Helsinki, located at MRC-CBSU. Data were digitized at 1 kHz with a high pass filter of cutoff 0.03 Hz. Head position was monitored continuously using four Head Position Indicator coils. Horizontal and vertical electrooculogram were recorded using two pairs of bipolar electrodes. One pair of bipolar electrodes were used to record electrocardiogram for pulse-related artifact removal during offline analysis.

The data presented here consisted only of resting state, where the subject sat still with their eyes closed for a minimum duration of 8 minutes and 40 seconds.

Data preprocessing

Preprocessed data was provided by Cam-CAN research consortium, where for each run temporal signal space separation was applied to remove noise from the environment, from Head Position Indicator coils, line noise and for the detection and reconstruction of the signal from noisy sensors. All the data had been transformed into a common head-position. More details about data acquisition and preprocessing have been presented elsewhere (Taylor et al., 2017; Shafto et al., 2014).

Data analysis

Welch spectrum

Fieldtrip toolbox (Oostenveld et al.,2011) was used to read the data provided in '.fif' format. For each individual, data was down sampled from 1 kHz to 250 Hz. First, we sought to investigate age specific changes in the spectral densities of the raw MEG signals.

Time series corresponding to the 102 magnetometers, resulted in a matrix X of size $102 \times T$, where Tcorresponds to number of time points. Power spectral density for each sensor c's time series $x_c(t)$ was estimated using Welch's periodogram method. Each time series was divided into segments of 20 seconds without any overlap between segments. Spectrum was estimated for each segment after multiplying it with a Hanning window. Spectrums of all the segments were finally averaged.

We estimated a global spectrum, representative of each subject i.e. $S_I(f)$ by taking a grand average across the spectrums belonging to all magnetometers.

$$S_I(f) = \sum_c S_I(c, f) \qquad (1)$$

Quantification of spatial overlap between sources of alpha and beta activity in the sensor space

For each subject, the sensor map of alpha and beta activity was normalized separately.

$$\hat{\alpha}_I(c) = \frac{\alpha_I(c) - <\alpha_I>}{\sigma_{\alpha(I)}} \qquad (2)$$

$$\hat{\beta}_I(c) = \frac{\beta_I(c) - <\beta_I>}{\sigma_{\beta(I)}} \qquad (3)$$

Separation between the normalized sensor level representation $\hat{\alpha}_I$and $\hat{\beta}_I$was indexed by the cosine angle between the two multidimensional vector spaces.

$$\theta(\alpha, \beta) = cos^{-1}\left(\frac{\hat{\alpha}_I . \hat{\beta}_I}{|\hat{\alpha}_I||\hat{\beta}_I|}\right). \qquad (4)$$

The angular separations across age were statistically analyzed using Spearman rank correlations and t-tests.

Global coherence

To measure the covariation of neural oscillations on a global level, we employed a technique known as global coherence (Cimenser et al., 2008; Kumar et al.,2016). Global coherence among sensors at any frequency f is measured as the percentage of variance explained by the first eigenvector of the cross spectral density matrix at f.

In an individual subject's data, for each sensor, the time series $x(t)$was divided into Nnon-overlapping windows of 5seconds duration each i.e. $y(t)$. This has resulted in an average of 112 (median, Interquartile range 1, range 70-220) windows for each subject. We considered 3 orthogonal discrete prolate spheroidal sequences, also known as Slepian tapers, to avoid leakage in spectral estimates into nearby frequency bands. The time-bandwidth product was taken to be 2, which resulted in a bandwidth of 0.4Hz.
Before computing FFT, each data segment was detrended i.e. from each data segment $y(t)$ the best straight-line fit was regressed out.

$$\hat{y}(t) = y(t) - \bar{y}(t) \qquad (5)$$

where $\underline{y}(t)$is the straight line fit of $y(t)$. Each segment was multiplied with a set of 3 orthogonal Slepian tapers and fast fourier transform was applied to the tapered segments. The resulting FFT values for the 3 tapered segments corresponding to the original detrended data segment $\hat{y}(t)$ were averaged.
Computing the complex FFT at frequency f for each segment $n$of sensor c resulted in a complex matrix $Y$of dimension $F \times C \times N$.

Cross spectral density between two sensors was estimated from $\hat{Y}$ by using the formula

$$S_f(i,j) = \frac{1}{N}\sum conj(\hat{Y}(f,i,n)) \times \hat{Y}(f,j,n) \qquad (6)$$

where $i$and $j$are the channel indices, f is the frequency index and n is the segment index.

Singular value decomposition was applied to the cross spectral density matrix $S_f$for each frequency value f.

$$S_f = USU^T \qquad (7)$$

Diagonals of Swould be proportional to the explained variance by the orthogonal set of eigenvectors U. The values of S were normalized so that each entry denote the percentage of the net variance explained in S_f.

$$\hat{S} = \frac{S}{\sum_i S_i} \quad (8)$$

The first entry of $\hat{S}$ is defined as the global coherence. Global coherence was computed for each frequency value f, resulting an array G of length F.

Metastability

We calculated the metastability measure for all participants across all magnetometer sensors. Metastability is defined as variability of the Kuramoto Order parameter,$R(t)$, which is given as,

$$R(t)e^{i\psi(t)} = \frac{1}{N}\left|\sum_N e^{i\phi_n(t)}\right| \quad (9)$$

Where $\varphi_n$is the phase of the n^{th} oscillator and ψ is the mean phase of the system of oscillators. In this analysis, every MEG sensor is conceptualized as a coupled oscillator, summarized by its instantaneous phase $\phi(t)$. At any given point of time, the phase of each oscillator is extracted and projected onto a polar coordinate system, as a unit vector ($e^{i\phi_n}$). The length of the resultant vector, obtained from summing all the unit vectors is interpreted as the Kuramoto Order parameter,$R(t)$. The temporal variability of R, as measured by the standard deviation, is taken to be the metastability (Deco et.al., 2017).

As a first step, the pre-processed resting state time series was band-pass filtered so as to obtain filtered time series. Instantaneous phase of each filtered band was estimated from the filtered data for metastability calculation. The pass band for the band-pass filtering step was kept narrow so that the resulting phase is readily interpretable.

For this analysis, each time series was filtered in the following 8 bands- 2-4 Hz, 3-7 Hz, 8-12 Hz, 12-16 Hz, 16-20 Hz, 20-24 Hz, 24-28 Hz and 28-32 Hz. As mentioned earlier, the choice of frequency bands was dictated by phase considerations. An additional criterion was to chunk the frequency bands so that they map onto well-known frequency bands such as delta, theta, alpha and beta. The beta band was further split into 5 smaller, non-overlapping bands. As mentioned earlier, we restricted our analysis to below 40 Hz due to presence of HPI noise.

FieldTrip toolbox (ft_preproc_bandpassfilter.m) was used to band-pass filter each signal in the appropriate frequency bands. This routine was used to implement a finite impulse response (FIR), two-pass filter that preserves phase information of the time series.

Subsequently, instantaneous phase was estimated by using built-in MATLAB implementation of the Hilbert transform (hilbert.m). The resulting phase time series for each channel and participant was used to calculate band and subject specific metastability.

Similar to the preceding analysis, metastability analysis was performed by a) treating age as a continuous variable, b) binning participants in the following age brackets - 18-35 years (Young Adults), 36-50 years (Middle Age), 51-65 years (Middle Elderly) and 66 -88 years (Elderly).

For the region-wise analysis, the brain was segmented into 5 non-overlapping regions (frontal, centro-parietal, occipital, left and right temporal). Metastability index was calculated individually for all regions separately by randomly sampling 14 sensors from each region. Metastability was tracked as a function of age by calculating the Spearman rank correlations.

Conclusions

In summary, our analysis maps out the spatiotemporal relationship of resting state spectral signals with healthy aging, specifically the importance of several frequencies in processing of brain signals. We demonstrate the age-related changes in global patterns of activity measured through global coherence and metastability, when interpreted concurrently reveals a comprehensive account of the neurophysiological changes with ageing. The most revealing aspect of this change is that no chosen frequency band is representative of the global brain dynamics, rather one needs carefully understand the relationships between different frequency bands. Mapping out such aspects of brain coordination dynamics should be the subject of future research, outcome of which can improve the accuracies of classifiers that aim to segregate healthy aging from neurodegenerative disorders, such as AD and Parkinson's disease.

Disclosure Statement

The authors declare no conflicts of interest.

Acknowledgements

This study was supported by NBRC Core funds, Ramalingaswami Fellowships (Department of Biotechnology, Government of India) to DR (BT/RLF/Re-entry/07/2014) and AB (BT/RLF/Re-entry/31/2011) and Innovative Young Biotechnologist Award (IYBA) to AB (BT/07/IYBA/2013). AB also acknowledges the support of Centre of Excellence in Epilepsy and MEG. DR was also supported by SR/CSRI/21/2016 extramural grant from the Department of Science and Technology (DST) Ministry of Science and Technology, Government of India. Data collection and sharing for this project was provided by the Cambridge Centre for Ageing and Neuroscience (CamCAN). CamCAN funding was provided by the UK Biotechnology and Biological Sciences Research Council (grant number BB/H008217/1), together with support from the UK Medical Research Council and University of Cambridge, UK.

References

Abeysuriya, R. G., Hadida, J., Sotiropoulos, S. N., Jbabdi, S., Becker, R., Hunt, B. A., ... & Woolrich, M. W. (2018). A biophysical model of dynamic balancing of excitation and inhibition in fast oscillatory large-scale networks. *PLoS computational biology*, *14*(2), e1006007.

Benjamini, Y., Hochberg, Y. (1995). Controlling the false discovery rate: A practical and powerful approach to multiple testing. J. R. Stat. Soc. Series B Stat. Methodol. 57, 289-300.

Bishop, N. A., Lu, T., & Yankner, B. A. (2010). Neural mechanisms of ageing and cognitive decline. *Nature*, *464*(7288), 529.

Bressler, S. L., & Kelso, J. S. (2001). Cortical coordination dynamics and cognition. Trends in cognitive sciences, *5*(1), 26-36.

Buzsaki, G.(2011) Rhythms of the brain. Oxford University Press

Cimenser,A.,Purdon,P.L.,Pierce,E.T.,Walsh,J.L.,Salazar-Gomez,A.F.,
Dave, S., Brothers, T. A., & Swaab, T. Y. (2018). 1/f neural noise and electrophysiological indices of contextual prediction in aging. *Brain research*, *1691*, 34-43.

Harrell,P.G., et. al.(2011).Tracking brain states under general anesthesia by
Using global coherence analysis. Proc.Natl.Acad.Sci.U.S.A. 108,8832–8837.

doi:10.1073/pnas

Clark, C. R., Veltmeyer, M. D., Hamilton, R. J., Simms, E., Paul, R., Hermens, D., & Gordon, E. (2004). Spontaneous alpha peak frequency predicts working memory performance across the age span. International Journal of Psychophysiology, *53*(1), 1-9.

Córdova-Palomera, A., Kaufmann, T., Persson, K., Alnæs, D., Doan, N. T., Moberget, T., & Engedal, K. (2017). Disrupted global metastability and static and dynamic brain connectivity across individuals in the Alzheimer's disease continuum. Scientific reports, *7*, 40268.

Davis, S. W., Dennis, N. A., Daselaar, S. M., Fleck, M. S., Cabeza, R. (2008). Que PASA? The posterior-anterior shift in aging. Cereb. Cortex. 18, 1201–1209.

Davis, S. W., Dennis, N. A., Buchler, N. G., White, L. E., Madden, D. J., & Cabeza, R. (2009). Assessing the effects of age on long white matter tracts using diffusion tensor tractography. *Neuroimage*, *46*(2), 530-541.

Deco, G., Jirsa, V.K., McIntosh, A.R. (2011). Emerging concepts for the dynamical organization of resting-state activity in the brain. Nat. Rev. Neurosci. 12, 43-56.

Deco, G., & Kringelbach, M. L. (2016). Metastability and coherence: extending the communication through coherence hypothesis using a whole-brain computational perspective. *Trends in neurosciences*, *39*(3), 125-135.

Deco, G., Cabral, J., Woolrich, M. W., Stevner, A. B., Van Hartevelt, T. J., & Kringelbach, M. L. (2017). Single or multiple frequency generators in on-going brain activity: A mechanistic whole-brain model of empirical MEG data. *Neuroimage*, *152*, 538-550.

Dickinson, A., DiStefano, C., Senturk, D., & Jeste, S. S. (2018). Peak alpha frequency is a neural marker of cognitive function across the autism spectrum. *European Journal of Neuroscience*, *47*(6), 643-651.

Duffy, F.H., Albert, M.S., McAnulty, G., Garvey, AJ. (1984). Age-related differences in brain electrical activity of healthy subjects. Ann. Neurol. 16, 430-438.

Foster, J. J., Sutterer, D. W., Serences, J. T., Vogel, E. K., & Awh, E. (2015). The topography of alpha-band activity tracks the content of spatial working memory. *Journal of neurophysiology*, *115*(1), 168-177.

Fotenos, A.F., Snyder, A.Z., Girton, L.E., Morris, J.C., Buckner, R.L. (2005). Normative estimates of cross-sectional and longitudinal brain volume decline in aging and AD. Neurology. 64, 1032-1039.

Fries, P. (2005). A mechanism for cognitive dynamics: neuronal communication through neuronal coherence. Trends Cogn. Sci. 9, 474-480.

Hall, S.D., Stanford, I.M., Yamawaki, N., McAllister, C.J., Rönnqvist, K.C., Woodhall, G.L., Furlong, P.L. (2011). The role of GABAergic modulation in motor function related neuronal network activity.

Hanslmayr, S., Aslan, A., Staudigl, T., Klimesch, W., Herrmann, C.S., Bäuml, K.H. (2007). Prestimulus oscillations predict visual perception performance between and within subjects. Neuroimage. 37, 1465-1473.

Heinrichs-Graham, E., McDermott, T. J., Mills, M. S., Wiesman, A. I., Wang, Y. P., Stephen, J. M., ... & Wilson, T. W. (2018). The lifespan trajectory of neural oscillatory activity in the motor system. Developmental cognitive neuroscience, *30*, 159-168.

Hellyer, P. J., Scott, G., Shanahan, M., Sharp, D. J., & Leech, R. (2015). Cognitive flexibility through metastable neural dynamics is disrupted by damage to the structural connectome. *Journal of Neuroscience*, *35*(24), 9050-9063.

Ishii, R., Canuet, L., Aoki, Y., Hata, M., Iwase, M., Ikeda, S., ... & Ikeda, M. (2017). Healthy and Pathological Brain Aging: From the Perspective of Oscillations, Functional Connectivity, and Signal Complexity. *Neuropsychobiology*, *75*(4), 151-161.

JF Hipp, DJ Hawellek, M Corbetta, M Siegel, AK Engel (2012) Large-scale cortical correlation structure of spontaneous oscillatory activity. Nature Neuroscience volume 15, pages 884–890.

Jeong, J. (2004). EEG dynamics in patients with Alzheimer's disease. Clin. Neurophysiol. 115, 1490-1505.

Kempermann, G., Kuhn, H.G., Gage, F.H. (1997). More hippocampal neurons in adult mice living in an enriched environment. Nature. 386, 493-505.

Koenig, T., Prichep, L., Lehmann, D., Sosa, P.V., Braeker, E., Kleinlogel, H., Isenhart, R., John, E.R. (2002). Millisecond by millisecond, year by year: normative EEG microstates and developmental stages. Neuroimage. 16, 41-48.

Kringelbach, M. L., McIntosh, A. R., Ritter, P., Jirsa, V. K., & Deco, G. (2015). The rediscovery of slowness: exploring the timing of cognition. *Trends in cognitive sciences*, *19*(10), 616-628.

Kumar, G. V., Halder, T., Jaiswal, A. K., Mukherjee, A., Roy, D. and Banerjee, A. (2016). Large scale functional brain networks underlying temporal integration of audio–visual speech perception: An EEG study, Front. Psychol. 7, 1558. DOI:10.3389/fpsyg.2016.01558.

Loerch, P. M., Lu, T., Dakin, K. A., Vann, J. M., Isaacs, A., Geula, C., ... & Prolla, T. A. (2008). Evolution of the aging brain transcriptome and synaptic regulation. *PloS one*, *3*(10), e3329.

Maurits, N.M., Scheeringa, R., van der Hoeven, J.H., de Jong, R. (2006). EEG coherence obtained from an auditory oddball task increases with age. J. Clin. Neurophysiol. 23, 395-403.

Muthukumaraswamy, S.D., Myers, J.F., Wilson, S.J., Nutt, D.J., Lingford-Hughes, A., Singh, K.D., Hamandi, K. (2013). The effects of elevated endogenous GABA levels on movement-related network oscillations. Neuroimage. 66, 36-41.

Naik, S., Banerjee, A., Bapi, R.S., Deco, G., Roy, D. (2017). Metastability in Senescence. Trends Cogn. Sci. 21, 509-527.

Osipova, D., Ahveninen, J., Jensen, O., Ylikoski, A., Pekkonen, E. (2005). Altered generation of spontaneous oscillations in Alzheimer's disease. Neuroimage. 27, 835-841.

Oostenveld, R., Fries, P., Maris, E., & Schoffelen, J. M. (2011). FieldTrip: open source software for advanced analysis of MEG, EEG, and invasive electrophysiological data. *Computational intelligence and neuroscience*, *2011*, 1.

Pesaran, B., Vinck, M., Einevoll, G. T., Sirota, A., Fries, P., Siegel, M., Truccolo, W., Schroeder, C. E.,Srinivasan, R. (2018) Investigating Large-Scale Brain Dynamics Using Field Potential Recordings: Analysis and Interpretation. *Nature Neuroscience*. **21**, 903–919.

Pfefferbaum, A., Sullivan, E. V., Hedehus, M., Lim, K. O., Adalsteinsson, E., & Moseley, M. (2000). Age-related decline in brain white matter anisotropy measured with spatially corrected echo-planar diffusion tensor imaging. *Magnetic Resonance in Medicine: An*

Official Journal of the International Society for Magnetic Resonance in Medicine, *44*(2), 259-268.

Pfurtscheller, G., Lopes da Silva, F.H. (1999). Event-related EEG/MEG synchronization and desynchronization: basic principles. Clin. Neurophysiol. 110, 1842-1857.

Purdon, P.L., Pavone, K.J., Akeju, O., Smith, A.C., Sampson, A.L., Lee, J., Zhou, D.W., Solt, K., Brown, E.N. (2015). The Ageing Brain: Age-dependent changes in the electroencephalogram during propofol and sevoflurane general anaesthesia. Br. J. Anaesth. 115, i46-i57.

Raz, N., Lindenberger, U., Rodrigue, K. M., Kennedy, K. M., Head, D., Williamson, A., ... & Acker, J. D. (2005). Regional brain changes in aging healthy adults: general trends, individual differences and modifiers. *Cerebral cortex*, *15*(11), 1676-1689.

Reuter-Lorenz, P.A., Jonides, J., Smith, E.E., Hartley, A., Miller, A., Marshuetz, C., Koeppe, R.A. (2000). Age differences in the frontal lateralization of verbal and spatial working memory revealed by PET. J. Cogn. Neurosci. 12, 174-187.

Rossini, P.M., Del Percio, C., Pasqualetti, P., Cassetta, E., Binetti, G., Dal Forno, G., Ferreri, F., Frisoni, G., Chiovenda, P., Miniussi, C., Parisi, L., Tombini, M., Vecchio, F., Babiloni, C. (2003). Conversion from mild cognitive impairment to Alzheimer's disease is predicted by sources and coherence of brain electroencephalography rhythms. Neuroscience. 143, 793-803.

Rossiter, H.E., Davis, E.M., Clark, E.V., Boudrias, M.H., Ward, N.S. (2014). Beta oscillations reflect changes in motor cortex inhibition in healthy ageing. Neuroimage. 91, 360-365.

Samaha, J., & Postle, B. R. (2015). The speed of alpha-band oscillations predicts the temporal resolution of visual perception. Current Biology, *25*(22), 2985-2990.

Samaha, J., Sprague, T. C., & Postle, B. R. (2016). Decoding and reconstructing the focus of spatial attention from the topography of alpha-band oscillations. *Journal of cognitive neuroscience*, *28*(8), 1090-1097.

Scally, B., Burke, M. R., Bunce, D., & Delvenne, J. F. (2018). Resting-state EEG power and connectivity are associated with alpha peak frequency slowing in healthy aging. *Neurobiology of aging*, *71*, 149-155.

Shafto, M.A., Tyler, L.K., Dixon, M., Taylor, J.R., Rowe, J.B., Cusack, R., Calder, A.J., Marslen-Wilson, W.D., Duncan, J., Dalgleish, T., Henson, R.N., Brayne, C., CamCAN, & Matthews, F.E. (2014). The Cambridge Centre for Ageing and Neuroscience (CamCAN) study protocol: a cross-sectional, lifespan, multidisciplinary examination of healthy cognitive ageing. BMC Neurology, 14(204). doi:10.1186/s12883-014-0204-1.

Soikkeli, R., Partanen, J., Soininen, H., Pääkkönen, A., Riekkinen, P.Sr. (1991). Slowing of EEG in Parkinson's disease. Electroencephalogr. Clin. Neurophysiol. 79, 159-165.

Stam, C.J., van der Made, Y., Pijnenburg, Y.A., Scheltens, P. (2003). EEG synchronization in mild cognitive impairment and Alzheimer's disease. Acta. Neurol. Scand. 108, 90-96.

Strunk, J., James, T., Arndt, J., Duarte, A. (2017). Age-related changes in neural oscillations supporting context memory retrieval. Cortex. 91, 40-55.

Taulu, S., Simola, J., Kajola, M. (2005). Applications of the signal space separation method. IEEE Trans. Signal Process. 53, 3359-3372.

Taylor, J.R., Williams, N., Cusack, R., Auer, T., Shafto, M.A., Dixon, M., Tyler, L.K., Cam-CAN, Henson, R.N. (2017). The Cambridge Centre for Ageing and Neuroscience (Cam-CAN) data repository: Structural and functional MRI, MEG, and cognitive data from a cross-sectional adult lifespan sample. NeuroImage. 144, 262-269.

Toepper, M. (2017). Dissociating normal aging from Alzheimer's disease: A view from cognitive neuroscience. *Journal of Alzheimer's Disease*, *57*(2), 331-352.

Tognoli, E., & Kelso, J. S. (2014). The metastable brain. *Neuron*, *81*(1), 35-48.

Uhlhaas, P.J., Singer, W. (2006). Neural Synchrony in Brain Disorders: Relevance for Cognitive Dysfunctions and Pathophysiology. Neuron. 52, 155-168.

Volf, N.V., Gluhih, A.A. (2011). Background cerebral electrical activity in healthy mental aging. Hum. Physiol. 37, 51-60

Voytek, B., Kramer, M. A., Case, J., Lepage, K. Q., Tempesta, Z. R., Knight, R. T., & Gazzaley, A. (2015). Age-related changes in 1/f neural electrophysiological noise. *Journal of Neuroscience*, *35*(38), 13257-13265.

Tables and Figures

Age group	N	% Female
YA (18-35)	126	55
ME (36-50)	159	49
ML (51-65)	149	50
OA (66-88)	216	46

Table1. Sample size and gender in each representative age group

A. Global spectrum of different age groups

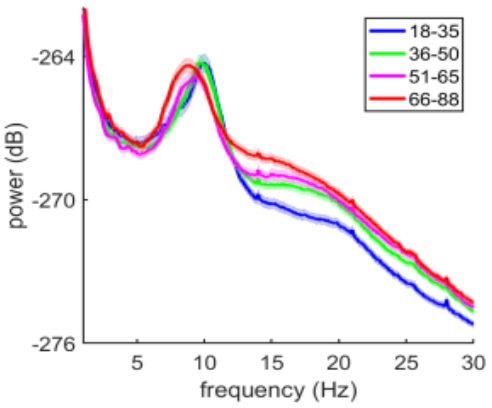

B. Variation in beta power with age

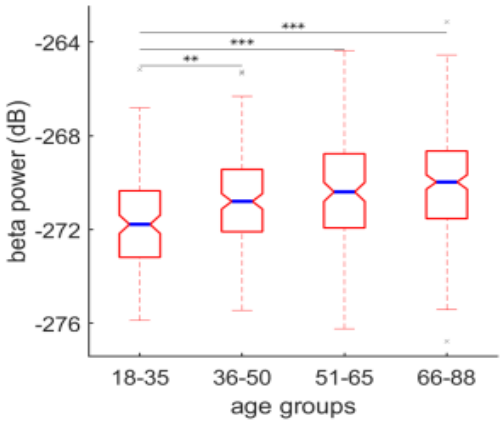

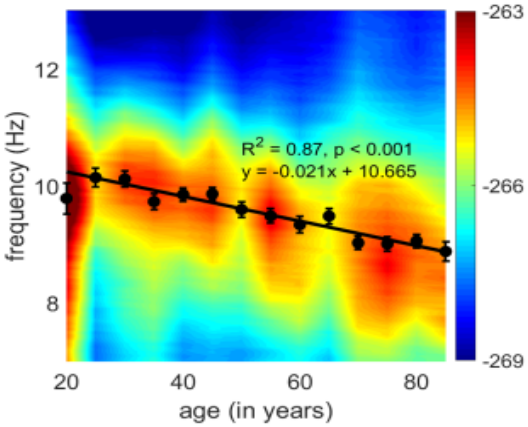

C. Spectrogram

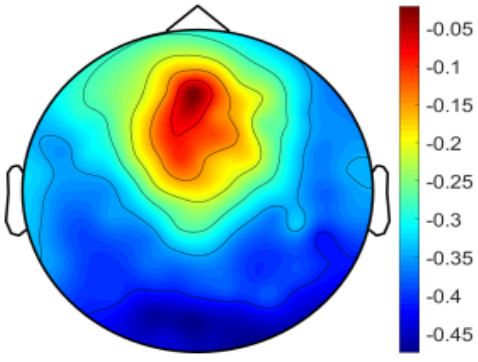

D. Correlation Topoplot

Figure 1. Relation between global spectral activity and age. A. Plots of mean power spectral density for 4 non-overlapping age groups i.e. 18-35, 36-50, 51-65 and 66-88. Shaded region denotes standard error of mean. **B.** Boxplot of distribution of band limited power in the beta band (16-25 Hz). Blue line indicates the median of each distribution. Notch denotes 95% confidence interval of the median. **C.** Variation of alpha activity with aging has been plotted as an age-spectrogram. Center frequency in the alpha band for each age bin has been plotted as solid circles and solid black line is the linear fit of these points **D.** Sensor topography of correlation between peak alpha frequency and age. Colorbar represents Spearman's rank correlation value.

A. Global coherence of different age groups

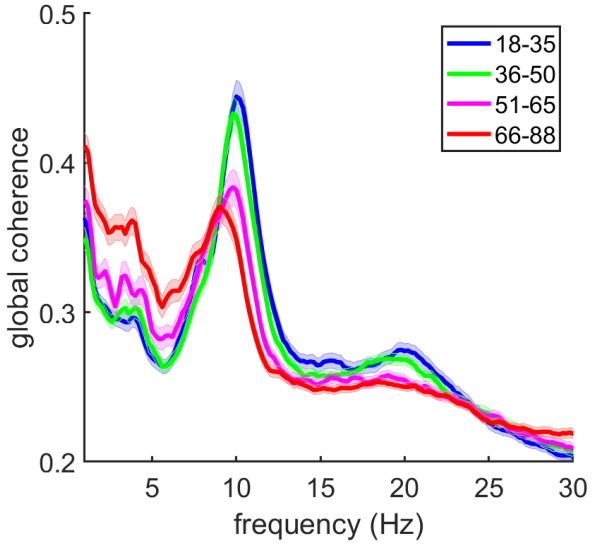

B. Global coherence of oscillations at slow and fast time scales

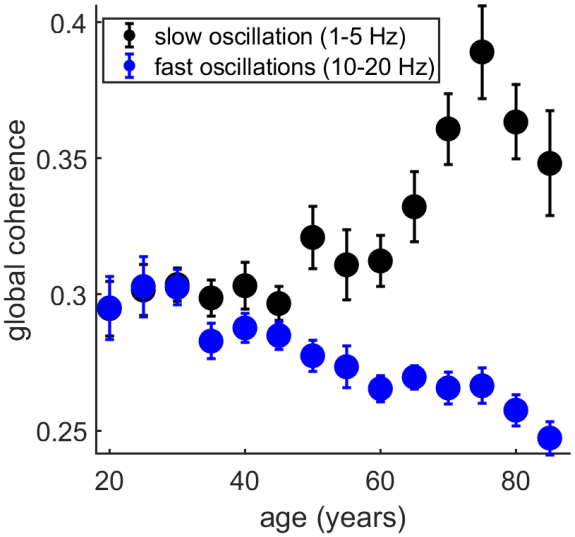

C. Global coherence in different frequency bands

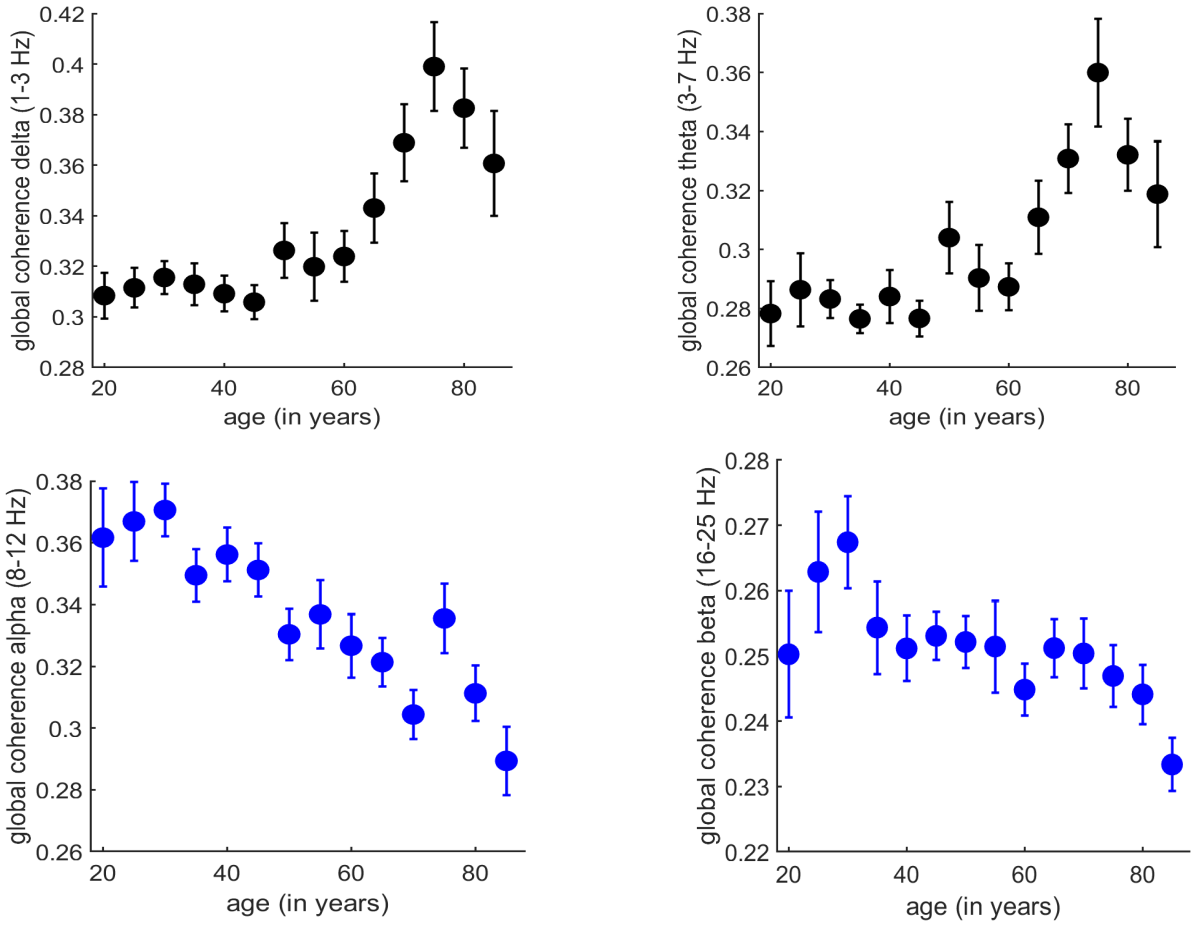

Figure 2. Differential changes in global coherence with aging. **A.** Plots of mean global coherency for the four age groups. Shaded region denotes s.e.m. **B.** Differential variation of global coherency for slow (1-5 Hz) and fast oscillations (10-20 Hz). **C.** Variation of global coherence with aging. Solid circle denotes the average global coherence value for a) Delta oscillations (1-3 Hz) b) Theta oscillations (3-7 Hz) c) Alpha oscillations (8-12 Hz) d) Beta oscillations (16-25 Hz) in each age bin of 5 years. Errorbar denotes s.e.m.

A. Topographical representation of alpha and beta power for OA and YA

B. Cluster of sensors showing differences between OA and YA

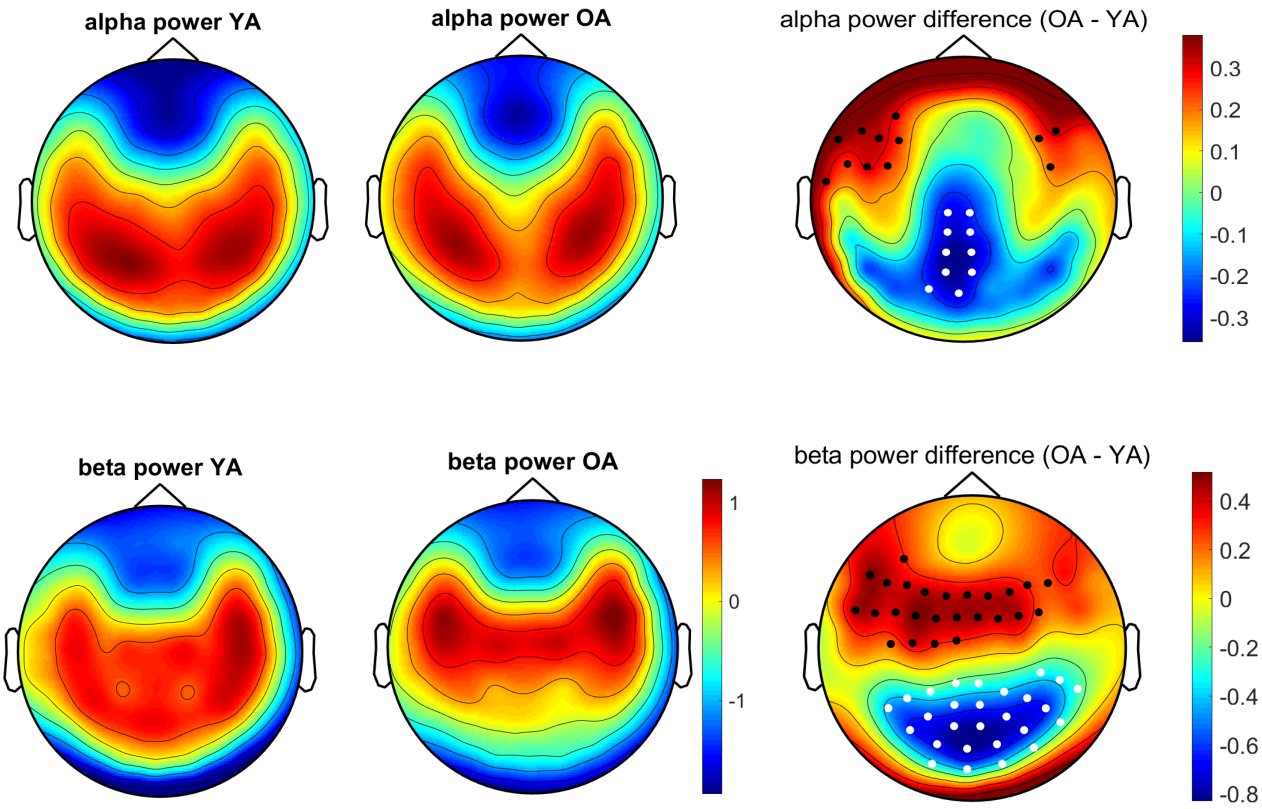

C. Variation in segregation of alpha and beta sensor map with aging

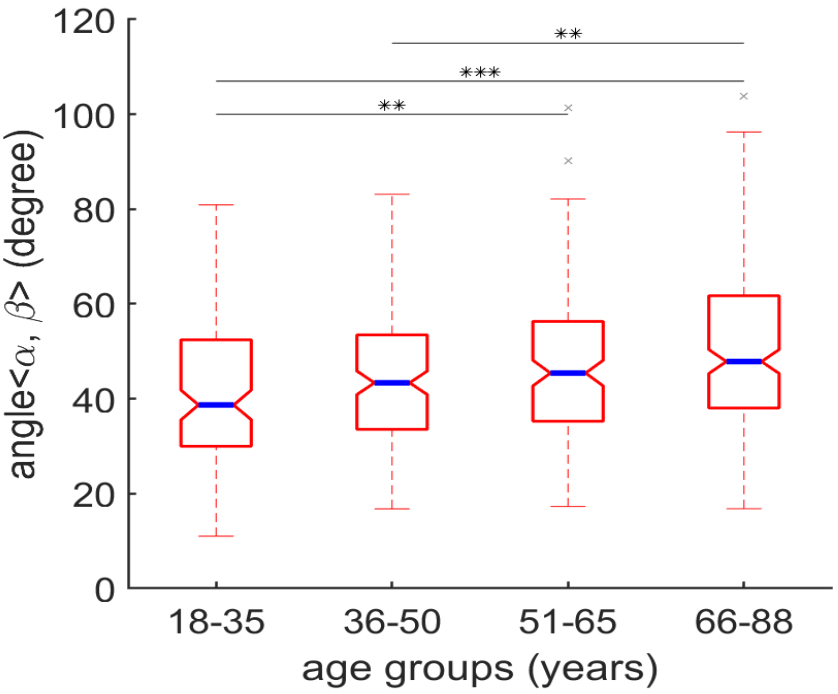

Figure 3. Segregation of sensor level topographies with aging. **A.** Sensor topographies of alpha power at center frequency and average beta power for the two extreme age groups. **B.** Clusters of sensors with significant differences in power between the oldest and youngest age group for alpha band (8-12 Hz) and beta band (16-25 Hz). White dots represent sensors with a negative difference and black dots represent sensors with a positive difference. **C.** Boxplot for the distribution of angles between the sensor topographies of center alpha power and average beta power for the four age groups. Blue line denotes the median of the distribution and the notch indicates 95% confidence interval of the median.

A. Metastability with Aging

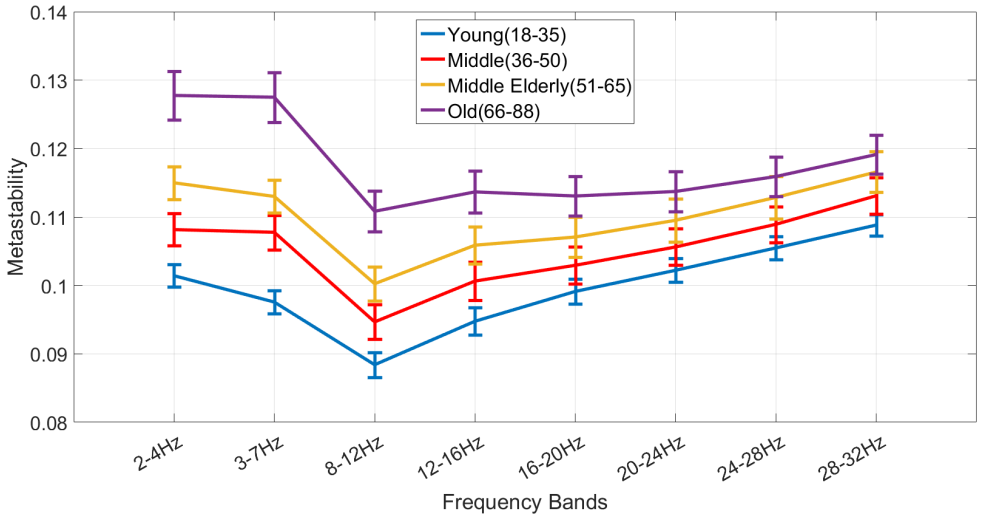

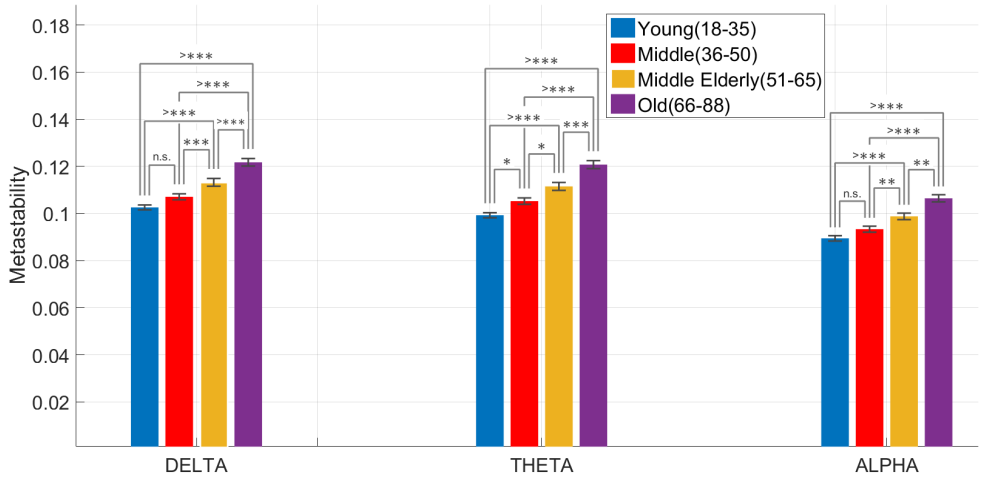

B. Band Specific Metastability

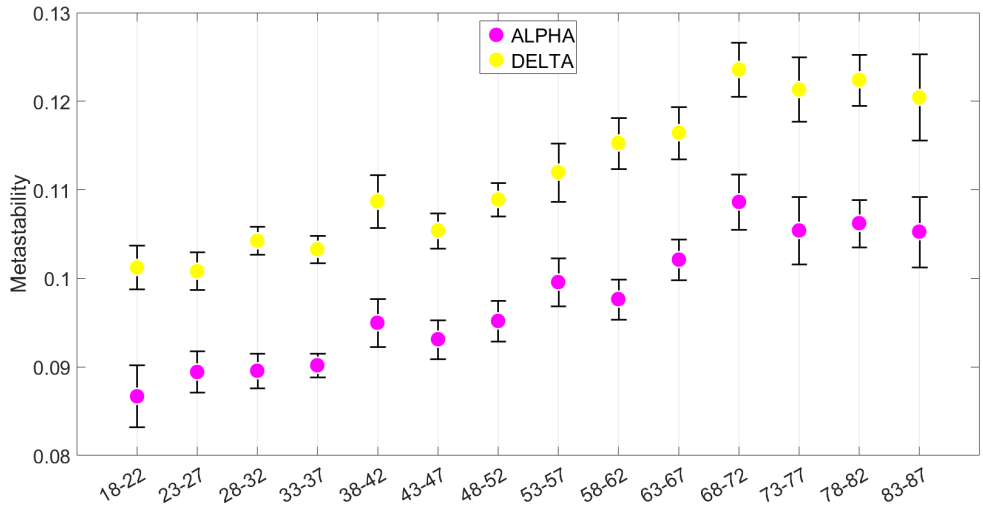

C. Metastability in smaller age groups

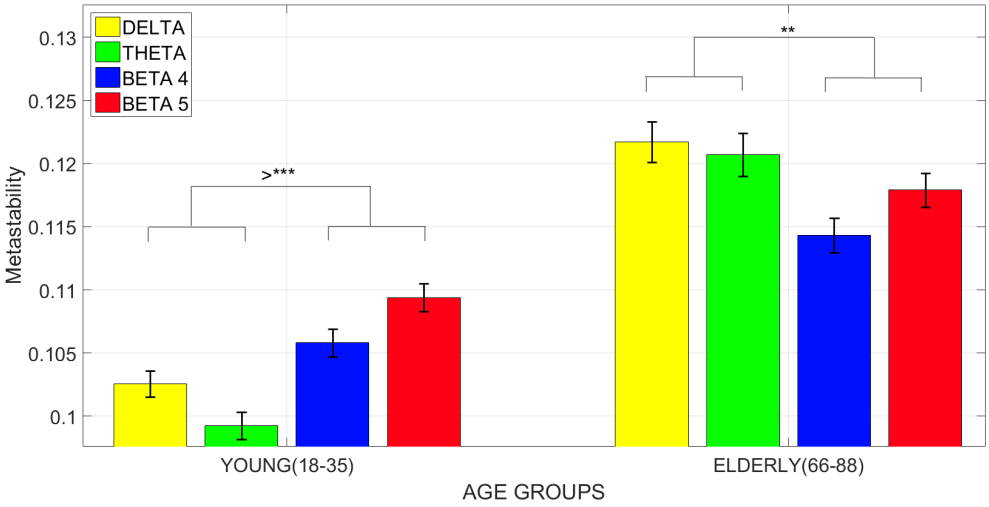

D. Slow vs fast time scales in metastability

Figure 4: Metastability across age groups. A. Metastability of four age groups. **B.** Metastability of the four age groups in the delta, theta and alpha bands. Stars between bars indicate statistical significance. **C.** Metastability across age groups divided into age bands of 5 years. **D.** Differential profiles of metastability in young vs old cohort. Statistical significance (indicated by stars) between slow frequencies (delta and theta) and fast frequencies- beta 4(24-28 Hz) and beta 5(28-32Hz) for single two-sample KS test.

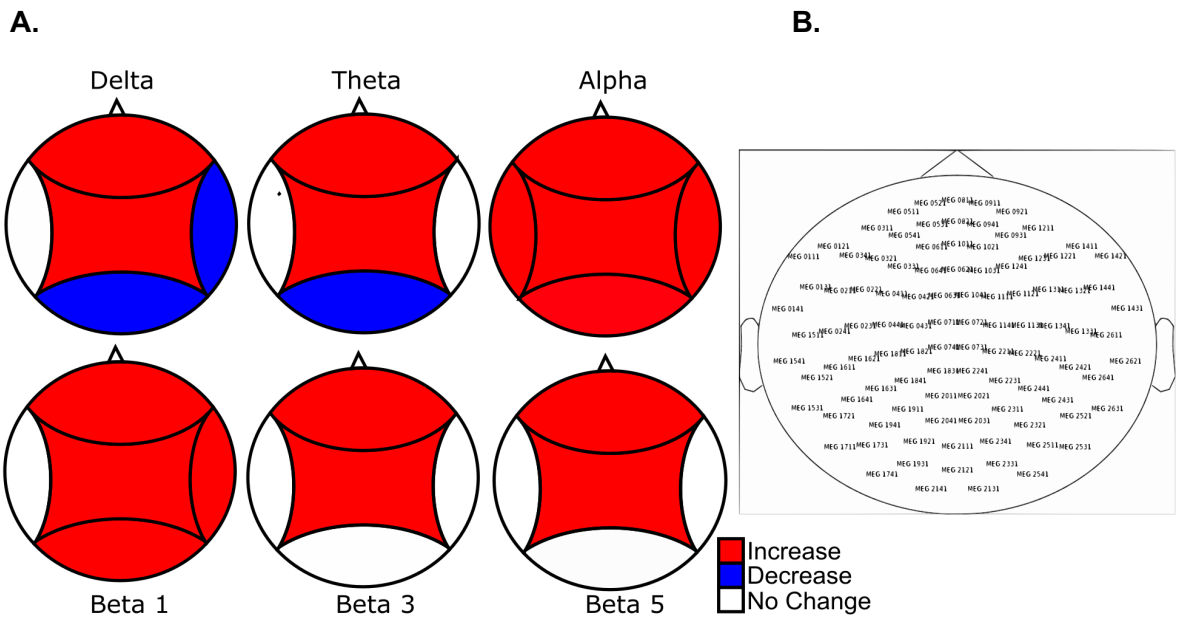

Figure 5: Region-wise increase and decrease in global metastability. A. Shows the results for the region-wise metastability analysis. Colors indicate the direction of the age-related trend as measured by the spearman rank correlation coefficients. 14 sensors were chosen at random from each of the 5 anatomical areas- frontal, centro-parietal, occipital, left and right temporal. **B.** Vector View magnetometer layout.